FMRFamide and Membrane Stretch as Activators of the *Aplysia* S-Channel

David H. Vandorpe,* Daniel L. Small,* Andre R. Dabrowski,‡ and Catherine E. Morris*
*Department of Biology, University of Ottawa, Neurosciences, Loeb Institute, Ottawa Civic Hospital, and ‡Department of Mathematics, University of Ottawa, Ottawa, Ontario, Canada

ABSTRACT The long-standing distinction between channels and transporters is becoming blurred, with one pump protein even able to convert reversibly to a channel in response to osmotic shock. In this light, it is plausible that stretch channels, membrane proteins whose physiological roles have been elusive, may be transporters exhibiting channel-like properties in response to mechanical stress. We recently described a case, however, where this seems an unlikely explanation. An *Aplysia* K channel whose physiological pedigree is well established (it is an excitability-modulating conductance mechanism) was found able to be activated by stretch. Here we establish more firmly the identity of this *Aplysia* conductance, the S-channel, as a stretch channel. We show that the permeation and fast kinetic properties of the stretch-activated channel and of the FMRFamide-activated S-channel are indistinguishable. We have also made progress in extending the kinetic analysis of the stretch channel to situations of multiple channel activity. This analysis implements a novel renewal theory approach and is therefore explained in some detail.

INTRODUCTION

Under single-channel recording conditions, the open probability of some channels alters when suction is applied to the recording pipette. Channels exhibiting this behavior ("stretch channels") may or may not act as physiological mechanotransducers. Although their physiological roles remain controversial (Gustin et al., 1991; Morris, 1992), stretch channels command attention because they occur in most cell types (Martinac, 1992; Morris, 1990; Sackin, 1993). How tension modifies the activity of certain membrane proteins without affecting others is unknown. Many plausible molecular mechanisms can be imagined, and it is probably inappropriate to expect that one explanation will encompass all cases. Membrane stretch is even a candidate for the factor that converts the multidrug pump to the volume-activated Cl channel (Gill et al., 1992); such a transformation would be more radical than the transitions generally envisaged in models of stretch activation (Lecar and Morris, 1993).

Some stretch channels may serve mechanosensory functions, such as modulating the membrane potential in response to the tension changes of a cleavage cycle (Medina and Bregestovski, 1991). For other channels, stretch-sensitivity may be adventitious (Morris and Horn, 1991). We recently demonstrated (Vandorpe and Morris, 1992), in identified mechanosensory neurons of the pleural ganglion of *Aplysia*, a stretch-sensitive K channel that exhibits many of the characteristics of stretch-activated K channels of neurons and heart cells from *Lymnaea stagnalis* (Sigurdson and Morris, 1989; Sigurdson et al., 1987). We found that this *Aplysia* channel was indistinguishable from the *Aplysia* mechanosensory neuron channel characterized as the "S-channel" by Siegelbaum and colleagues (1982). Named for its modulation by serotonin, the S-channel is also sensitive to the peptide neurotransmitter, FMRFamide, which activates it via an arachidonic acid pathway (Belardetti et al., 1987). Here we provide further evidence that the *Aplysia* mechanosensory neuron stretch-activated K channel is the serotonin- and FMRFamide-sensitive K channel.

Stretch and the FMRFamide pathway represent radically different activating stimuli for the S-channel; whether their effects converge on a single gating mechanism is not clear. We explore this issue by comparing kinetically identifiable states induced by FMRFamide and by stretch. In kinetic analyses of stretch channels, a recurrent problem is that of dealing with several simultaneously active channels. We have therefore tested a new analysis program designed to reveal several kinetic aspects of multiple ion channel patches (Dabrowski and McDonald, 1992). First the program tests the stationarity of multiple channel data to determine its suitability for further analyses that are based on the binomial distribution of current levels. The program then assesses whether the channel events contributing to a stationary section of data appear independent and identical. This process includes estimating (*a*) the number of channels in the patch, (*b*) open probability, (*c*) global means for open and closed times, and (*d*) cumulative open and closed time distributions.

Received for publication 7 July 1993 and in final form 20 September 1993.

Address reprint requests to Dr. Catherine E. Morris, Neurosciences, Loeb Institute, 1053 Carling Avenue, Ottawa Civic Hospital, Ottawa, Ontario, Canada K1Y 4E9. Tel.: 613-761-5073; Fax: 613-761-5330.

Dr. Vandorpe's present address is Department of Physiology, Dartmouth Medical School, Hanover, NH 03755.

0006-3495/94/01/46/13 $2.00

MATERIALS AND METHODS

Identified mechanosensory neurons from the pleural ganglion of *Aplysia californica* in primary culture were used 1 to 3 days after plating (Lin et al., 1989; Vandorpe and Morris, 1992). Single channel recordings were made from cell-attached or excised inside-out patches, as indicated, using an Axopatch 1-D amplifier (Axon Instruments). Pipettes were fabricated from borosilicate glass (N51A, OD 1.65 mm ID 1.15 mm; Garner Glass, Claremont, CA) and pulled using a List L/M-3PA puller (Darmstadt, FRG).

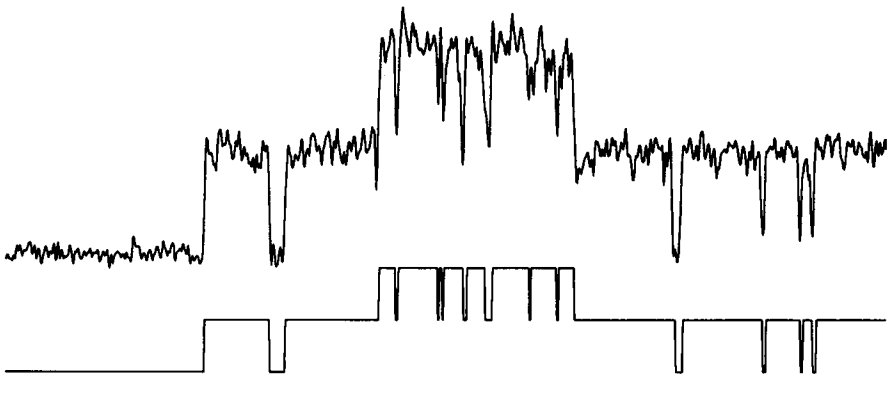

Chunk	1	2	3	4	5	6
Downstep Vector	0, 0	1, 0	0, 1	0, 5	1, 2	3, 0
Occupation Density	1,0,0	.48,.52,0	0,.71,.29	0,.10,.90	.02,.73,.25	.09,.91,0
Average Level	0	.52	1.29	1.90	1.23	0.91

FIGURE 1 Illustration of preliminary data analysis by the program, ADaM. The figure deals with a small subset of data; a 100 ms-trace of raw current record is shown with its idealized record underneath. Data is typically divided into several hundred or up to a maximum of 1000 chunks of time. Six chunks of 15.43 ms duration are shown. They were analyzed to yield downstep vectors, occupation density vectors, and the average levels. Downstep vectors contain a string of integers 0, 1 $\cdots$ z, (in this case 0 $\cdots$ 5) representing the number of downsteps per chunk from the current levels 1 $\cdots$ n (in this case, 1, 2; n is the highest current level visited during the entire analysis period). Occupation density vectors contain a string of real numbers, $0 \leq \times \leq 1, \Sigma = 1$, representing occupation densities for the current levels 0 $\cdots$ n (in this case 0, 1, 2). Average level (for which the single channel current level has been normalized to 1) is computed from the occupation density data. The chunk duration should be chosen so that on average at least two downsteps are observed in each chunk.

Resistances of the pipettes filled with *Aplysia* salines were in the range 1–8 Mohms. The pipette holder's sideport was connected to a pressure transducer (Biotek Instruments, Winooski, VT). In some on-line experiments, a signal from the transducer was sent to one channel of the computer's A/D convertor.

Unless otherwise indicated, pipette solutions were comprised of 460 mM NaCl, 10 mM KCl, 10 mM HEPES, 11 mM $CaCl_2$, 55 mM $MgCl_2$, and 10 mM TEA chloride, pH 7.6. The bath solution (NAS) was the same, pH 7.4, but with no TEA. In experiments involving FMRFamide (Phe-met-arg-phe-amide) (Sigma, St. Louis, MO) induced channel activity, a 20 μM solution was perfused by macropipette over the patched cell. 100 μM serotonin hydrochloride (5-HT) (Sigma) was applied in the same manner (Belardetti et al., 1986, 1987) in some experiments. Any solution changes during an experiment were effected by changing the bath by perfusion with a macropipette.

To block the activity of Ca^{2+}-activated K channels (Shuster et al., 1991), we routinely used 10 mM TEA chloride in pipette solutions. The K_d for TEA block of *Aplysia* Ca^{2+}-activated K channels is 0.4 mM (Shuster et al., 1991). Permeability experiments with thallium employed the following pipette solution: 50 mM thallium acetate, 1 mM TEA acetate, 1 mM $CaHPO_4$, and 5 mM HEPES, pH 7.6. Immediately before the experiment, in order to prevent precipitation of thallium chloride in the pipette tip, the bath was changed from normal *Aplysia* saline to 470 mM Na acetate, 11 mM calcium acetate, 10 mM HEPES, pH 7.4.

V_p, the pipette potential, is reported. V_{rest} for these cells in normal saline is usually about −45 mV (Baxter and Byrne, 1990).

Channel currents were usually recorded on video tape (Sony, beta) after pulse code modulation (PCM-1; bandwidith 0–16 khz; Medical Systems Corp., Greenvale, NY). Currents were analyzed by replaying the tape through an eight-pole Bessel filter (2 kHz; Frequency Devices, Haverhill, MA) connected to a microcomputer via a Labmaster A/D interface. Single-channel events were digitized at 10 kHz with FETCHEX, event lists produced with FETCHAN (FETCHAN uses a 50% threshold criterion for capturing events), and histograms generated with pSTAT, subroutines of the software package pCLAMP v5.5.1 (Axon Instruments). Given that the digitizing frequency was 5 × the filter frequency, the 2 kHz filter constituted the final effective cutoff frequency and the deadtime for event detection was about 90 μs (that is, 0.9 times the sample interval of 100 μs) (see Colquhoun and Sigworth, 1983, p. 217). No correction for missed events has been applied. Subconductance events were rare (as indicated by visual inspection of the records and from point-by-point amplitude histograms) in the recordings that we used for one-channel kinetic analysis and so misassignments associated with such events were ignored. pSTAT's nonlinear, least squares curve-fitting method was used to fit gaussian and exponential functions to the data. In a few cases, currents were recorded on-line via the A/D interface using FETCHEX.

Closed time analysis was conducted by fitting three components to the square root ordinate versus log dwell time histogram (Sigworth and Sine, 1987).

Results are reported as means ± standard error, except where indicated. Paired or unpaired t-tests and χ^2 distributions were used, where appropriate.

ADaM Analysis

For some experiments that yielded current records with several simultaneously active channels, events lists generated by FETCHAN, as above, were analyzed by the program ADaM. The ADaM Channelyzer is a set of computer programs that implement the statistical techniques for ion channel kinetic analysis (Dabrowski et al., 1990; Dabrowski and McDonald, 1992) and is available from A. Dabrowski or D. McDonald (Department of Mathematics, University of Ottawa). This program allows the analysis of multiple channel records from which information about the average duration of open and closed sojourns of individual channels is not normally obtained. ADaM uses current level, occupation density, and downstep data (see Fig. 1) for the following purposes: to test for stationarity and then to provide estimates of N, the number of channels in a patch, of P_{open}, the open probability of a single channel, of τ_o, the mean open time of single channel events, and of τ_c, the mean closed time of single channel events (these means are global averages for *all* the open or closed states of the individual channel, regardless of how many kinetically distinct open or closed states might exist). In certain cases, estimates of open and closed time cumulative

probability distribution functions $F(t)$ and $G(t)$, respectively, can also be generated by the program. We examined only estimates of $F(t)$ and, in keeping with convention, plotted the corresponding (estimated) survival function, $1 - F(t)$.

More explicitly, ADaM uses the idealized multichannel current record to produce a sequence of data vectors as illustrated in Fig. 1. As in the case of single-channel data, statistical stationarity of the record over the period of observation is a prerequisite for analysis of its kinetics.

Within ADaM, both first and second order stationarity tests were conducted on multiple channel patches. First order stationarity simply requires that the mean behavior of a process (current density and number of downsteps per unit time) remains constant over time, whereas the second-order stationarity requires that the variances and lag covariances (a lag(t) covariance is the covariance of a process $X(s)$ with itself t seconds later, $X(t + s)$) of the process remain constant over time (Dabrowski and McDonald, 1992). ADaM provides tests on first- and second-order stationarity based upon a Kolmogorov-Smirnov-type test.

The test of independent and identical channels used by ADaM was a goodness of fit test (Dabrowski and McDonald, 1992) rather than, for example, a likelihood ratio method (as used in Belardetti et al., 1987). The goodness of fit approach is more robust, since it does not assume that the probability law governing the random variable is known (Larsen, 1974). If the ion channels in the patch are independent and identical, then the proportion of time that the total current record spends at each current level follows a binomial probability distribution with parameters N and P_{open}. This is true regardless of the precise probability law governing each channel. ADaM also uses the downstep rates in its analysis; this additional information permits the estimation of τ_o (and hence, of τ_c via the relation $P_{open} = \tau_o/(\tau_o + \tau_c)$) in addition to N and P_{open}.

ADaM estimates a covariance matrix of occupation times at the various levels, and the rate of downsteps from these levels. This matrix is used to define a quadratic form (expression 1 ref.; Dabrowski and McDonald, 1992) in terms of the unknown values of N, P_{open} and τ_o. The values that minimize this quadratic form and that conform to a model of independent and identical channels (i.e., a binomial structure) are our estimators of N, P_{open}, τ_o and τ_c. The value of the quadratic form evaluated at this point is our test statistic, and measures the statistical distance between our data and a best-fitting model of independent and identical (iid) channels. Under this null hypothesis, the test statistic has a chi-squared distribution. For data found to be comprised of the activity of iid channels, these estimates are used in a further stage of analysis to estimate the functions, $1 - F(t)$ and $1 - G(t)$.

A central feature of ADaM is that it explicitly tests the assumptions that the channels contributing to a multichannel record are, within a given level of confidence, iid. Given the nature of multichannel records (they contain much less time-sequence information than single-channel records), a limitation imposed on the ADaM approach is that open states are aggregated or lumped together, as are the closed states. From single-channel records, it is possible to estimate the number of states and rate constants of each state. In a multichannel setting, this is much more difficult. ADaM is not so ambitious, and attempts only to estimate τ_o (τ_c), the global mean open (closed) time. In the likely event that the channel has more than one open (closed) state, the mean open (closed) time, this τ_o (τ_c) is the average length of all open (closed) periods. Nonetheless, ADaM's ability to estimate these global means represents an improvement on just being able to estimate channel numbers and channel open probability.

ADaM implements the methods of Dabrowski and McDonald (1992), which is an improvement on Dabrowski et al. (1990). Whereas Dabrowski et al. (1990) use the amount of time spent by the overall current record at levels 0, 1, 2 . . . etc., Dabrowski and McDonald (1992) use both these data and the record of downstep transitions. Regardless of the kinetic scheme of the channel, the record of current level occupation and transitions may be used to estimate the unknown parameters.

RESULTS

Identity of SAK Channel as the S-Channel

Aplysia mechanosensory neurons exhibit both SAK channel activity and S-channel activity; the two classes of events probably represent activity of the same channel entity (Vandorpe and Morris, 1992). The following data provide further support for this conclusion.

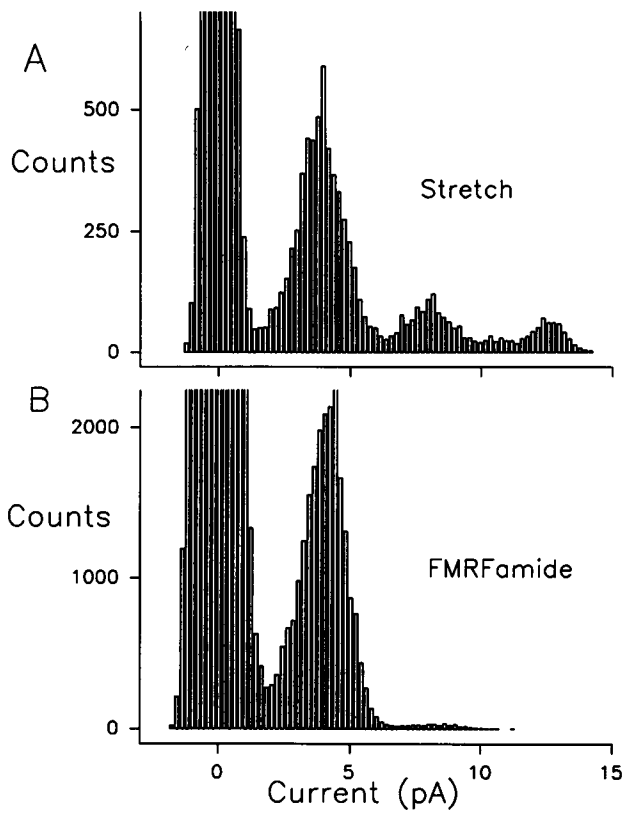

FIGURE 2 Amplitude histograms illustrating stretch-activated (A) and FMRFamide induced events (B) in the same patch at the same pipette potential. The mean currents of the first open level were 4.6 ± 0.3 and 4.5 ± 0.6 pA, respectively, ($p > 0.05$). This histogram is associated with patch 1 of Table 1 A.

S-channel activity is inducible by FMRFamide, and if FMRFamide-induced events and SAK events represent currents through the same population of channels, then in any given patch, channels stimulated first by FMRFamide and then by stretch should exhibit the same current amplitudes for the same membrane potential. Fig. 2 shows amplitude histograms for stretch-activated (A) and FMRFamide-induced (B) currents in the same patch at the same pipette potential. In keeping with FMRFamide's relatively feeble S-channel activating ability (see Belardetti et al., 1987) by comparison to that of stretch (Vandorpe and Morris, 1992), the point-by-point histogram for FMRFamide indicates almost exclusively single amplitude openings, whereas double and triple amplitude openings are common in the stretch histogram. Table 1, A and B, summarizes the data for six such patches. Note that the apparent number of channels activated by FMRFamide never exceeded the apparent number activated by stretch. Current amplitudes for stretch and FMRFamide were not statistically distinguishable. (Amplitudes were obtained by using pSTAT's gaussian fitting routine on the amplitude data representing the first open level; the errors listed in Table 1 are the errors associated with the fits).

TABLE 1 Comparison of the effect of FMRFamide and stretch on patch parameters

Patch No.	V_p	Apparent N		Single channel current (pA)		NP_{open}	
		N_{str}	N_F	Stretch	FMRF	Stretch	FMRF
A. 470 mM K and 10 mM TEA in pipette							
1	−100	3	2	4.5 ± 0.6	4.6 ± 0.3	0.17	0.06
2	−100	3	2	4.2 ± 0.7	4.7 ± 0.4	1.2	0.08
3	−100	1	1	2.7 ± 0.3	2.5 ± 0.23	0.03	0.02
B. 50 mM Tl and 1 mM TEA in pipette							
4	−100	2	2	4.8 ± 0.9	4.8 ± 1.2	0.20	0.03
5	0	1	1	2.4 ± 0.9	1.7 ± 0.2	0.08	0.001
6	−80	1	1	3.3 ± 0.2	2.8 ± 0.5	0.10	0.012

V_p, pipette potential in mV. N_{str}, number of stretch-activated channels. N_F, number of FMRFamide-activated channels. Single channel currents activated by stretch and FMRFamide were not different from each other in either group. ($p > 0.05$, by paired t test).

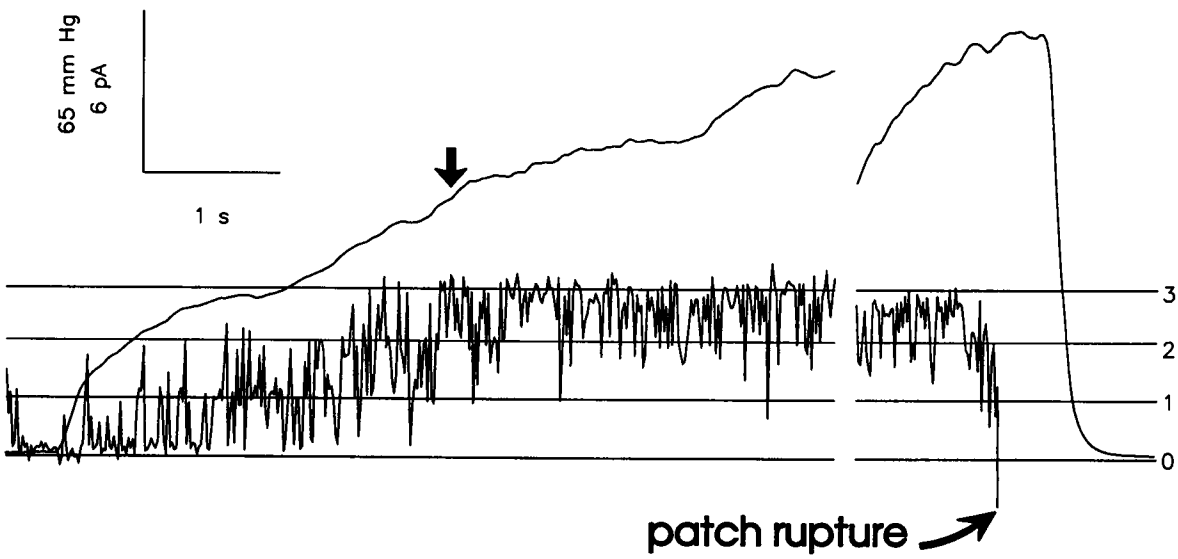

FIGURE 3 Saturation of stretch-activation. The current record indicates a maximum of three channels activated by suction (negative mm Hg indicated upward). The smoother trace is applied suction; beyond the downpointing arrow, suction was supramaximal. As the record beyond the interruption indicates, the membrane ruptured at −175 Hg.

Stretch-Induced Channel Activity Is Saturable

Because molluscan neuron patches often rupture at pressures not much greater than those that steeply activate the channels, it is ill-advised, on a routine basis, to directly determine N, the number of stretch-activated channels in a patch, by applying supersaturating levels of suction. In a previous report (Vandorpe and Morris, 1992), only nonsaturating stretch-activation curves for the S-channel were shown because, in each exeriment, rupture preceded saturation. This leaves the impression a) that saturation might not be possible and b) that the reported density of 1–4 stretch-activated channels per patch could have been considerably underestimated. Fig. 3 illustrates that activation is, indeed, stretch-saturable, and that when saturation is achieved, N is not outside the range reported on the basis of the maximum number of simultaneously active channels observed at subsaturating suction. For activation curves (Vandorpe and Morris, 1992), we used suction of fixed intensity for several seconds per intensity. Saturation is more readily achieved using continually increasing suction for several seconds as shown here, where the number of simultaneously open channels saturated at three. Although N can be rapidly checked by such supersaturating suctions (see Bedard and Morris, 1992), the risk of patch rupture is still considerable. In the illustrated case, the patch was especially robust. It ruptured at 175 mm Hg suction whereas many rupture at <100 mm Hg.

Thallium Currents in SAK and FMRFamide Channels

If FMRFamide-induced events and stretch events represent currents carried by different channels, it would be unlikely for the permeability characteristics of events activated by the different stimuli to match precisely. We presented the channels with a nonphysiological permeating ion and provided it at a concentration that, for *Aplysia*, is unusually low. Any idiosyncracies of distinct K channels should emerge in the form of distinctly shaped I/V relations. The ion used was thallium. The concentration was almost 10-fold lower than the monovalent cation concentrations in *Aplysia* salines, and Mg^{2+} was excluded (see Methods). Such a solution supports substantial currents in another stretch-sensitive molluscan

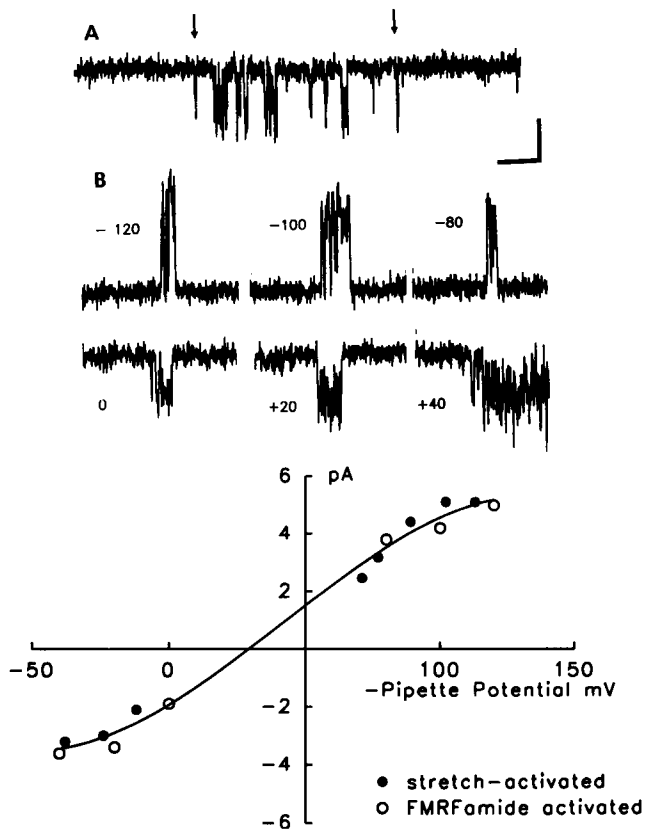

FIGURE 4 I/V "fingerprint" of the S-channel. (*A*) Inward thallium currents elicited by stretch (−110 mm Hg applied between the arrows; V_p, 40 mV). (*B*) FMRFamide induced events at the indicated V_p. (*C*) Example of an I/V relationship of stretch-activated and FMRFamide-induced events in the same patch. Note that the line fitted by eye serves well for both sets of points.

K^+ channel (Morris and Sigurdson, 1989). Fig. 4 illustrates the results of an experiment on a cell-attached patch in which the pipette solution contained 50 mM thallium acetate (1 mM TEA was included). This patch, and two others that were tested showed an increase in activity after perfusion of the cell with FMRFamide. FMRFamide increased NP_{open} by an average of eightfold, similar to what we previously reported (Vandorpe and Morris, 1992). Fig. 4 *A* shows the inward thallium currents elicited by the application of suction and Fig. 4 *B* gives examples of FMRFamide-induced events recorded at the indicated pipette potentials. As shown in Fig. 4 *C*, the I/V relations of FMRFamide-induced events and stretch-activated events were indistinguishable. This was also the case for the I/V relations of two other patches tested in the same way.

Kinetics of Stretch-Activated Events

Kinetic analysis of stretch-sensitive channels indicates that stretch-sensitivity resides not in an open-to-closed transition, but rather in transitions leading toward open states (e.g., Guharay and Sachs, 1985; Sigurdson et al., 1987). In effect, stretch markedly decreases the proportion of long closed intervals in any record without substantially affecting the duration of open intervals. Analysis at several activating pressures from two patches from *Aplysia* neurons that contained only one stretch-activated channel (such patches are rare) and whose P_{open} increased substantially with suction confirms that this is also the case for the S-channel (see Fig. 5). In these patches, the probability density functions could be best fit with the sum of two exponentials for the open events and three for the closed events. We used the Akaike information criterion to confirm that we were justified in using the two (as opposed to one or three) and three (as opposed to two or four) component fits (Horn, 1987; Landaw and Distefano, 1984). Fig. 5 shows that the only substantial effect of applied suction was to decrease the longest closed time. The kinetic characteristics of the *Aplysia* SAK channel are thus very similar to those observed for *Lymnaea* neurons (Sigurdson and Morris, 1989).

Comparison of Kinetics during Stretch and FMRFamide Activation

Fig. 6 shows open time histograms of FMRFamide-induced and stretch-activated events from the same patch at the same pipette potential. In this and two other patches in which first FMRFamide and then stretch-activated events were generated, the faster and slower open time constants were not significantly different (faster: 0.20 ± 0.01 versus 0.19 ± 0.02 ms and slower: 0.85 ± 0.19 versus 0.82 ± 0.21 ms, for FMRFamide and stretch, respectively; $n = 3$, $p > 0.05$ by paired *t*-test). Three time constants could be fitted to the closed time histograms. These were 0.26 ± 0.7, 1.2 ± 0.2, and 44 ± 6 ms for FMRFamide histograms and 0.16 ± 0.11, 0.8 ± 0.5, and 7 ± 3 ms for stretch. Of the three, only the slowest (third) closed time differed significantly between FMRFamide and stretch ($p < 0.05$).

Thus, when assessed under otherwise identical conditions (same patch, pipette potential, recording solutions, filter settings, fitting routine), stretch-activated and FMRFamide-induced events produced nearly identical kinetic "fingerprints"; they had the same collection of kinetic states (two open, three closed), and the faster of states were kinetically indistinguishable, in spite of differences in the prevailing open probability. Since the open probablity was higher during stretch than during FMRFamide induced activity, it is not surprising that FMRFamide's slowest time constant (the constant that largely determines the open probability during stretch activation) exceeded that for stretch.

Multiple Channel Kinetics: Stationarity

The spontaneously active S-channel is noted for its tendency to exhibit nonstationary kinetics (Siegelbaum et al., 1982), a tendency representing gating mode shifts among lower and higher open probability modes. Nonstationarity has hindered attempts at kinetic analysis of this channel. Fig. 7 illustrates a 4-s piece of stationary data from a patch that showed a high level of spontaneous activity and that contained at least three S-channels; the record passed the stationarity tests incorporated in ADaM. Subsequent binomial analyses were carried

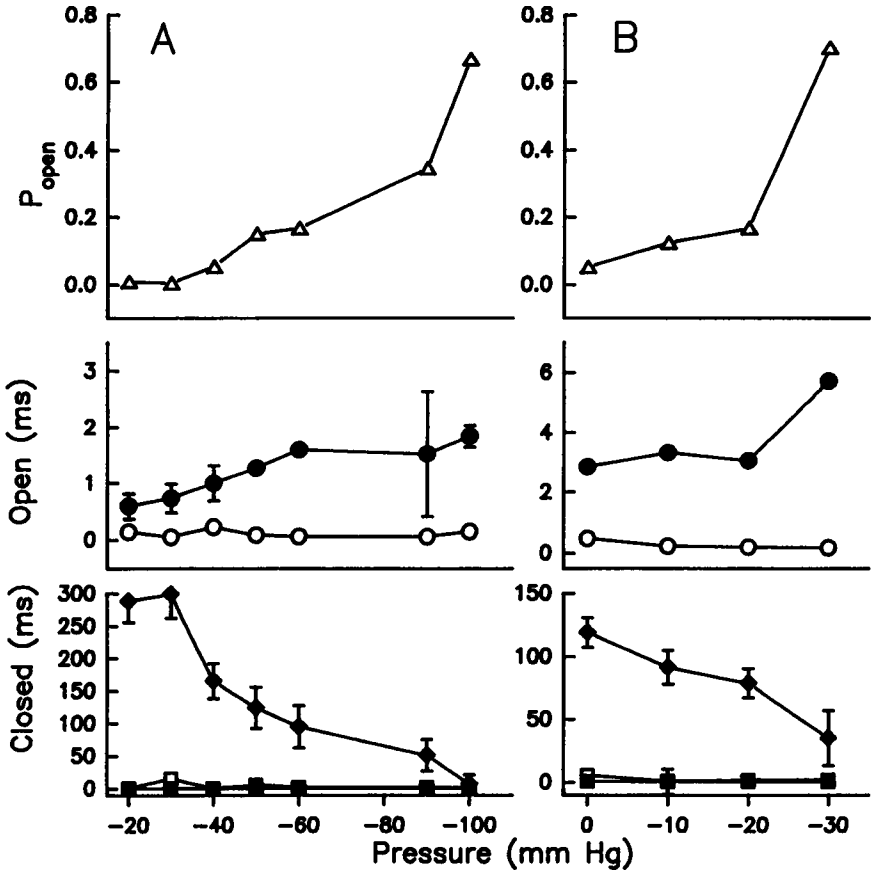

FIGURE 5 Kinetic analysis of stretch-activated events for two one-channel patches. Top panels show the effect of suction on P_{open}. Middle panels give the open time constants as a function of suction, with empty and solid circles corresponding to the fast and slow time constants, respectively. Bottom panels give the closed time constants as a function of increasing suction. Empty boxes, solid boxes, and solid diamonds correspond to the first, second, and third (longest) closed time constants, respectively. Patch A: cell-attached; V_p, −70 mV; NAS and TEA in pipette, NAS in bath. Patch B: excised patch; V_p, 0 mV; NAS and TEA in pipette, high K in bath.

out on such records if they passed first order and second order stationarity tests. However, it is worth recalling that individual channels in a given multichannel patch could be in different gating modes. If, say, two simultaneously active channels persisted in their different modes of activity, and a sufficiently long record was analyzed, the record would be deemed stationary. At the next level of analysis, however, ADaM would (within established confidence limits) detect that the channels contributing to the record were not independent and *identical.*

Stationarity over Different Time Scales

The question of which sections of a multichannel record are likely to be usable for kinetic analysis is tricky. Our experience was that it is difficult to tell by inspection of the current trace whether a given section of record of S-channel activity will prove stationary, presumably because of the slow processes that shift the channels among modes. Fig. 8 (and Table 2) illustrates an objective method for finding stationary stretches of data. ADaM generates two cumulative functions that are related to the number of downsteps in a given chunk of time and the average current level per chunk of time. The downsteps function, $\sum (D(t) - \bar{D}(t))$, represents the cumulative sum of the difference between the number of downsteps in chunk t and the mean number of downsteps in all chunks up to chunk t. Likewise the levels function, $\sum (L(t) - \bar{L}(t))$, represents the cumulative sum of the difference between the mean level in chunk t and the mean level in all chunks up to chunk t (Dabrowski and McDonald, 1992). These cumulative sums, plotted over the period under consideration, are useful for searching for stationary subsections of data. The rule of thumb is that over the regions where the slope of the plots for both functions are roughly constant, the record should pass the first order stationarity test. Table 2, Part 1 shows that this was the case for sections A, B, C in Fig. 8. D and E are examples of sections of the record that did not pass a first order stationarity test. Section E is comprised of the two contiguous stationary sections, B and C. It is as if the channels have undergone a mode change at the point at which the slopes of the two function plots change. Sections A, B, and C also passed second order stationarity tests that require that the variances and lag covariances of the two cumulative functions remain constant over time. Therefore, scanning the plots of the cumulative functions visually for constant slope provided a guide to

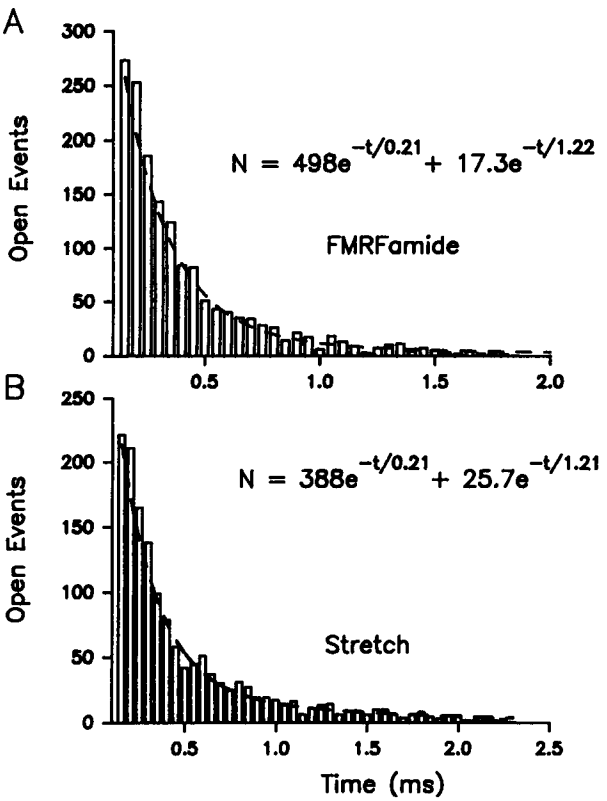

FIGURE 6 Open time histograms of FMRFamide and stretch-activated events in the same patch. The dashed lines overlying the bins indicate the probability density function: $N = W_1/\tau_1(\exp(-T/\tau_1))dt + W_2/\tau_2(\exp(-T/\tau_2))dt$, where T is the center value of a given bin width dt, τ_n is the respective time constant, W_n is the width of the nth term, and N is the number of counts in the given bin contributed by the term. V_p, −100 mV; 470 mM KCl and 10 TEA Cl in pipette, NAS in bath. Suction, −30 mm Hg.

stationarity that was far superior to visual inspection of raw data. Note that this general approach to the evaluation of stationarity is also applicable to records with only one patch active.

Numbers of Channels in Patch Activated by Suction

The process of estimating the number of channels in a patch subjected to 40-mm Hg suction is illustrated in Fig. 9. Before the application of suction, the activity of only one channel was apparent, while the application of suction resulted in the simultaneous activity of two channels in the patch. A binomial analysis conducted on this section of data supported the hypothesis that two independent and identical channels were operant.

From one-channel patch recordings of stretch channel data obtained at different applied suctions, it is by definition the case that suction increases P_{open} and not N. The ADaM analysis on multichannel recordings permits a wider range of possibilities, in that P_{open} and N could both potentially change. We expected to confirm that only P_{open} increases in patches subjected to suction. Disappointingly, an analysis of several patches (Table 3) indicated that increased NP_{open} in patches subjected to increased suction could be associated with a combination of changes: increased P_{open} only (patches 1, 2), increased N and P_{open} (patch 3) and increased N, marginally decreased P_{open} (patch 4). This array of possibilities convinced us that multiple-channel kinetic analysis of stretch channels (for example, to test stretch-sensitivity under various conditions) should not be undertaken without full binomial rigor. As Sokabe and Sachs (1990) have shown, patch suction is a problematic stimulus; sometimes it increases membrane area (potentially increasing N), other times, it causes vesicles to bud off (potentially decreasing N). Given these complications, it is understandable that the outcome of the present binomial analysis of stretch activation of the S-channel does not yield a story as straightforward as that associated with FMRFamide activation (Belardetti et al., 1987), in which NP_{open} changes were ascribed solely to increased P_{open}.

Open Channel Sojourns: Within-Patch Similarities of S-Channel and SAK Channel Activity

Consistent with the idea that SA K events and FMRFamide-induced events arise from the same channel population—the S-channels—was an analysis of activity in the only two patches (Table 4, *A* and *B*, and Fig. 10) we obtained whose FMRFamide-induced and spontaneous activity, along with their stretch activity, were adequate for ADaM analysis.

Fig. 10 *A* shows, for a given patch, the estimated cumulative open distributions ($F(t)$, plotted as the more familiar survival function, $1 - F(t)$) of FMRFamide and stretch activated events, respectively. Fig. 10 *B* compares spontaneous activity that was subsequently abolished by serotonin (5-HT), and stretch-induced activity recorded several minutes after 5-HT washout. The solid lines are estimates of $1 - F(t)$ for a *single* channel, based upon the estimates of N and P_{open} obtained by ADaM in its test of independent and identical channels, and upon the lengths of time spent by the multichannel record at varying current levels. The τ_o listed in Table 4 represents the mean open time for a single channel and is related to $F(t)$ by $\tau_o = \int_0^\infty F(t)\,dt$. Should the channel have but a single open state, $\hat{F}(t)$ would be an exponential function of mean τ_o; $\tau_o = \int_0^\infty t(1\backslash\tau_0)(\exp(-t/\tau_0))\,dt$. Dotted lines in Fig. 10 represent an estimate of $1 - \hat{F}(t)$, for a hypothetical (but unlikely) case where a single open state with closing rate $1/\tau_o$ is assumed. Although the estimator $\hat{F}$ and the estimated F (as given by ADaM; see Methods) have the same τ_o, it is clear for all cases in Fig. 10 that, not surprisingly, the single open-state model given by $\hat{F}$ is not a good model for the F estimated by ADaM.

This issue can, however, be pursued a step further by examining the exponential substructure of the F estimates plotted in Fig. 10 (that is, the estimated open time histograms for single-channel activity contributing to the multichannel record). Are they, like the true one-channel records, double exponentials? The last two columns in Table 4 indicate

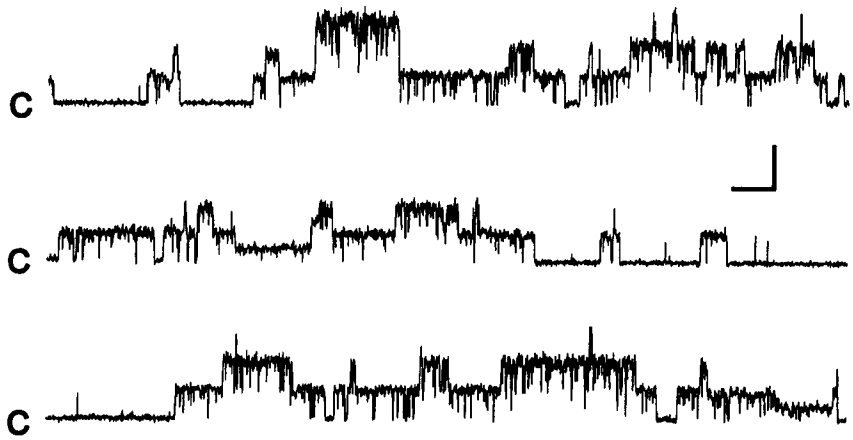

FIGURE 7 Four-second trace of spontaneous, stationary channel activity from a patch containing at least three channels. The first order stationarity test reported mean current level of 0.8, with $p = 0.29$. Average downstep frequency was 2.0, with $p = 0.53$ ($p < 0.05$ indicates that the data are nonstationary). Scales, 50 ms, 5 pA. C, zero-current level.

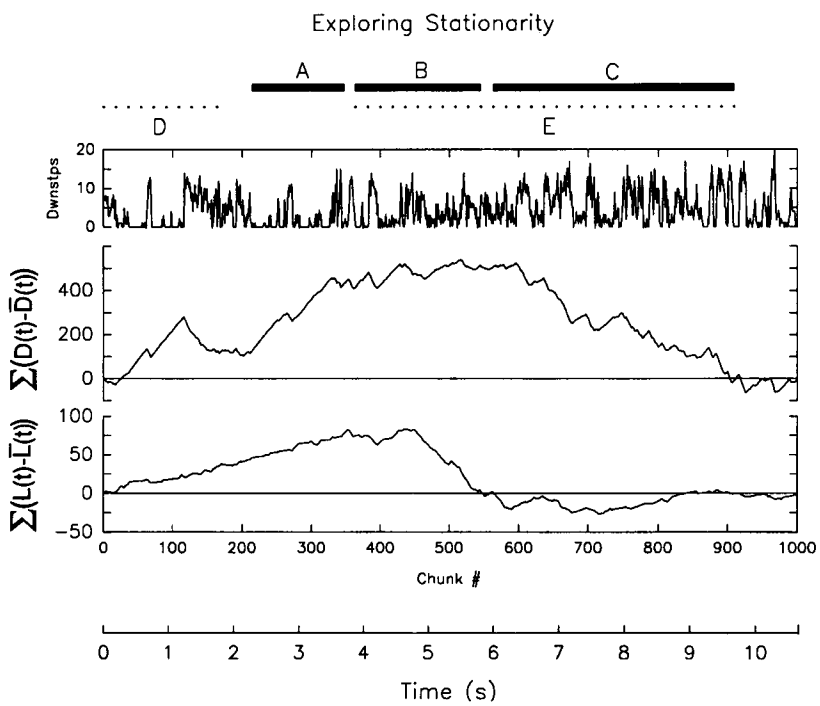

FIGURE 8 Exploring stationarity. This figure illustrates the procedure adopted to search for segments of record likely to be stationary. About 11 s of record with multichannel activity were digitized and divided into 1000 chunks. The upper plot of downsteps/chunk summarizes channel activity over this period. The two plots below show the evolution, with time, of the cumulative downstep function and the cumulative levels functions for the data. Using the rule of thumb described in the text, we predicted that data stretches A, B, and C would be stationary, whereas D and E would not. Table 2A indicates that these predictions were borne out. Note that segment E was not stationary, even though it encompasses two briefer stationary segments. The table also illustrates that segment C, though stationary, did not meet the criteria for independent and identical channels, and thus could not be used for further analysis.

that each estimated $1 - F(t)$ curve is well fit by two exponentials. In both patches and in all four conditions (stretch, FMRFamide, spontaneous, and post 5-HT stretch), τ_{o1} was the same–just under 1 ms. In the stretch/FMRFamide patch, τ_{o2} was indistinguishable for both modes of channel activation. Qualitatively, this pattern resembles the outcome from the direct one-channel analysis (i.e., two open times whose values are the same whether stretch or FMRFamide activate the channel), but quantitatively the time constants obtained by the one- and multichannel methods cover different ranges. The multichannel analysis detects a state of duration (τ_{o2}) intermediate to the two resolved by one-channel analysis, plus a longer-lived state. Note that, inevitably, multichannel data are severely censored in a way that makes estimation of slow states poorer than with single-channel data. The most direct utility of these data is, therefore, for making within-patch comparisons for different test conditions, and not for establishing absolute kinetic parameters.

TABLE 2 Exploring stationarity

Part 1. Cumulative plots and stationarity

	Interval (s)	$\bar{D}(t)$	$\bar{L}(t)$	$p\{D\}$	$p\{L\}$	Stationarity 1st order	Stationarity 2nd order
A	2.4–3.8	2.1	0.9	0.36	0.45	Y	Y
B	4.0–6.0	2.0	1.6	0.13	0.21	Y	Y
C	6.2–9.9	2.0	1.0	0.69	0.23	Y	Y
D	0.0–1.8	2.0	0.84	0.005	0.91	N	—
E	4.0–9.9	3.0	1.2	0.17	0.004	N	—

$\bar{D}(t)$ and $\bar{L}(t)$ are evaluated over the indicated time interval.
To pass 1st order stationarity, p values associated with both D and L cumulative functions must be <0.05.

Part 2. Fitting stationarity data and doing binomial test

	τ_o	τ_c	P_{open}	N	StdQ*	iid C?
A	3.7	8.5	0.30	3	2.5	Y
B	4.3	1.7	0.71	3	4.2	Y
C	2.0	4.5	0.30	3	44	N

* The values of the χ^2 test statistic, the standard quotient (StdQ) are compared with the value of the 95% critical point of a chi-squared distribution with 2 degrees of freedom (the value is 6.0). If this ratio is <1, then the binomial hypothesis of independent and identical channels (iid C) is accepted.

Although confidence bands are not provided for the estimates of $1 - F(t)$ by ADaM, visual comparison of both sets of estimated $1 - F(t)$ curves (see the almost completely overlaid curves in the Fig. 10 insets) support the idea that for each patch (A and B), the two cases are the same. In other words, channels in Patch A that contributed FMRFamide-induced open events to the first multichannel record had the same kinetic properties as those that subsequently contributed stretch-induced open events to the second multichannel record. Likewise for patch B; here, the spontaneous (subsequently shown to be 5-HT-inhibitable) and stretch-activated multichannel records yielded remarkably similar $1 - F(t)$ estimates. These within-patch $1 - F(t)$ similarities are consistent with the earlier conclusion (one-channel kinetics section) that SA K channels are S-channels and that, in activating the S-channel, stretch does not noticeably affect the length of its open channel sojourns. The multistep ADaM analysis that yields an estimated $1 - F(t)$ curve is, recall, carried out entirely independently for each experimental condition. Thus, when two independently determined curves (the estimated curves are sawtoothed; see Appendix) from one patch prove to be indistinguishable (as in A) or extremely alike (as in B), the similarity is not trivial. These visual "fingerprint" comparisons do not, of course, constitute a statistical hypothesis test. Nevertheless, taken together and in conjunction with the one-channel patch analysis, they make it a notch harder to dismiss the conclusion that the stretch-activated channel is the S-channel.

DISCUSSION

We recently reported that in *Aplysia* mechanosensory neurons, a K channel whose activity responds to FMRFamide and 5-HT is also sensitive to stretch (Vandorpe and Morris, 1992). This led us to conclude that the so-called S-channel (Shuster et al., 1991) is a stretch-activated K channel analogous to those in other molluscan neurons. In light of the prodigious ability of neurons to make K channel variants, our conclusion warranted closer inspection. To counteract problems of patch-to-patch variability, we compared permeation and kinetic traits of channels activated by FMRFamide and by stretch in a given mechanosensory neuron patch. 5-HT reduces S-channel activity in a "knock-out" fashion (Belardetti et al., 1987), so it is not possible to compare 5-HT-inhibited channels with stretch-activated channels in a parallel manner.

TABLE 3 AdaM anaysis: effect of stretch on '*N*' in multichannel patches

Patch No.	Pressure (mm Hg)	NP_{open}	N	P_{open}	τ_o (ms)	τ_c (ms)	StdQ
1	−30	0.66	3	0.22	8.1	27	1.6
1	−40	1.4	3	0.47	5.6	6.4	0.23
2	−40	1.2	3	0.40	6.3	9.3	1.2
2	−50	1.4	3	0.45	8.1	9.9	0.80
3	−20	1.3	5	0.26	4.4	13	1.6
3	−30	2.2	7	0.31	2.5	5.4	5.6
4	−40	1.1	3	0.35	5.5	10	3.1
4	−50	1.3	4	0.32	5.4	12	0.26

N, number of channels in patch. p_{open}, single channel open probability. τ_o, global average open time. τ_c, global average closed time. StdQ, the chi-squared statistic is <6 in each case (see Table 2) indicating that the null hypothesis (that the cannels were identical and independent) was tenable in each case.

Permeation Properties of Stretch and FMRFamide Activated Channels in the Same Patch

For distinct K channel proteins, details of permeability profiles are idiosyncratic. Hence, two distinct K channels in the same patch are not likely to have identical I/V relations when a mix of monovalent cations is present, especially considering that nonpermeant as well as permeant cations contribute to shaping I/V curves. Molluscan SA K channels pass no measurable Na current, but intracellular Na, acting as a nonpermeant blocker, affects the I/V relation by diminishing inward K currents (Bedard and Morris, 1992). Our earlier conclusion (Vandorpe and Morris, 1992) that S-channels and *Aplysia* SA K channels are the same entity was based on a general observation, namely, that for a given potential in a given patch, S-channels and SA K channels have indistinguishable unitary currents. That point is now made quantitatively (Table 1), but to press the issue, we examined the whole I/V relation for SA K and S-channels from the same patch. The recording solution was chosen to emphasize idiosyncracies of distinct K channels. Extracellular Tl (plus 1 mM TEA) was provided at a concentration (50 mM) roughly comparable to intracellular Na and low relative to cytoplasmic K (measured by Eaton et al. to be 61 mM and 280 mM, respectively in Aplysia neurons (Eaton et al., 1975)). The

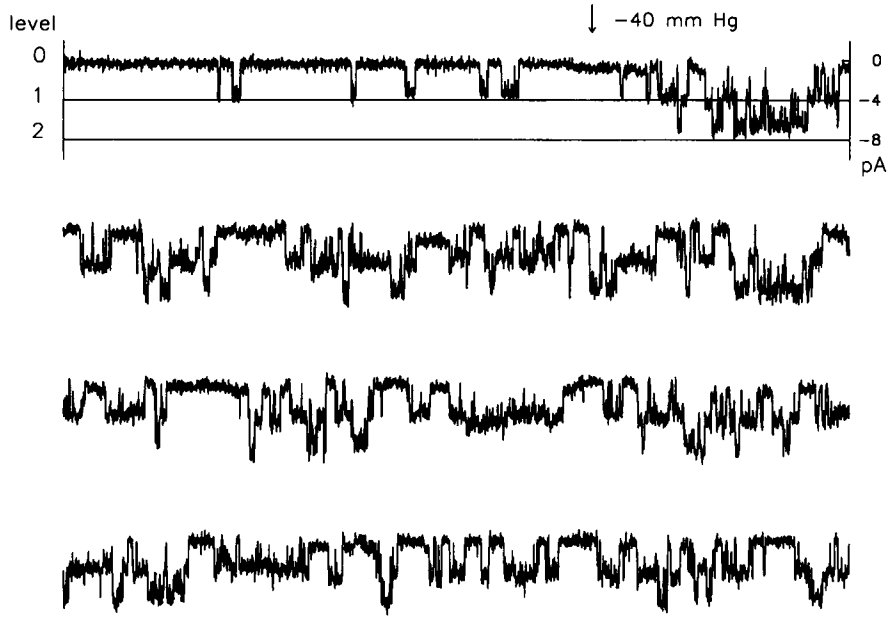

FIGURE 9 Multichannel record showing the effect of suction. ADaM analysis indicated two independent and identical channels during application of −40 mm Hg suction. V_p, −100 mV, NAS and 10 TEA in pipette, NAS in bath.

TABLE 4 ADaM analysis: binomial fits of FMRFamide, spontaneous and stretch activity

	No. type	N	P_{open}	τ_o (ms)	τ_c (ms)	StdQ	τ_{o1} (ms)	τ_{o2} (ms)
Patch A								
FMRFamide	1	3	0.23	2.2	7.4	1.7	0.7	6.1
Stretch	1	3	0.27	1.8	4.9	0.01	0.7	6.0
Patch B								
Spontaneous	1	4	0.26	2.6	7.5	1.5	0.5	15
Stretch (post 5-HT)	1	3	0.47	2.1	2.5	2.3	0.5	31

No. type, number of kinetically distinct kinds of channels, as determined in ADaM fit. N, number of channels. P_{open}, probability of being open. τ_o, global average open time. τ_c, global average closed time. StdQ, chi-squared statistic (as in Table 2) indicating that the null hypothesis (that the channels were identical and independent) was tenable in each case. τ_{o1} and τ_{o2} are time constants (done outside ADaM using Sigmaplot nonlinear curve-fitting routine) from double exponential fits to the $1 - F(t)$ curves. The error bounds associated with these time constants were all ≤5% except for one (31 ms) which was 15%.

shape of the nonlinear I/V relation and its position along the voltage axis (and hence the reversal potential) did not change when channels were stimulated first via FMRFamide then with stretch. This is good evidence that they are the same channel type–the S-channel.

The I/V relations are almost linear near the reversal potential, indicating inward Tl currents and outward K currents of nearly equal magnitude in the face of a roughly 6-fold Tl:K concentration gradient (see Fig. 4). The S-channel (i.e., FMRFamide/SA K channel) therefore, had a considerably bigger conductive permeability for Tl than K. The reversal potential for these conditions was more than 25 mV positive to the resting potential, also consistent with $P_{Tl} \gg P_K$. For two other types of K channels from molluscan neurons, P_{Tl}:P_K ratios close to unity have been reported (Gorman et al., 1982; Reuter and Stevens, 1980).

Kinetics of FMRFamide- and Stretch-Activated S-Channels

Under cell-attached single channel recording conditions, bath-applied FMRFamide was a relatively weak activator of S-channel activity compared with patch-applied stretch. In other words, the high concentration of FMRFamide used yielded NP_{open} values substantially smaller than those associated with moderate suction. Yet, regardless of whether the activating stimulus was FMRFamide or stretch and regardless of the intensity of stretch, S-channels exhibited, within the limits of our analysis, an identical number of kinetic states: five. These states were comprised of four relatively short-lived states (two open states, two closed states, all in the millisecond range) that were statistically indistiguishable when FMRFamide and stretch were compared, and a long closed state (tens to hundreds of milliseconds). The long closed state was affected by changes in the intensity of stretch, and varied depending on the NP_{open} value of the channels in the patch.

The simplest interpretation is that, stimulation, whether by stretch or by the arachidonic acid metabolite in the FMRFamide/lipoxygenase pathway (Buttner et al., 1989), increases the probability that the channel leaves a stable closed state (that characterized by the longest closed time constant) to enter a "flickery" mode (the set of states that produce the short open and closed time constants). Because

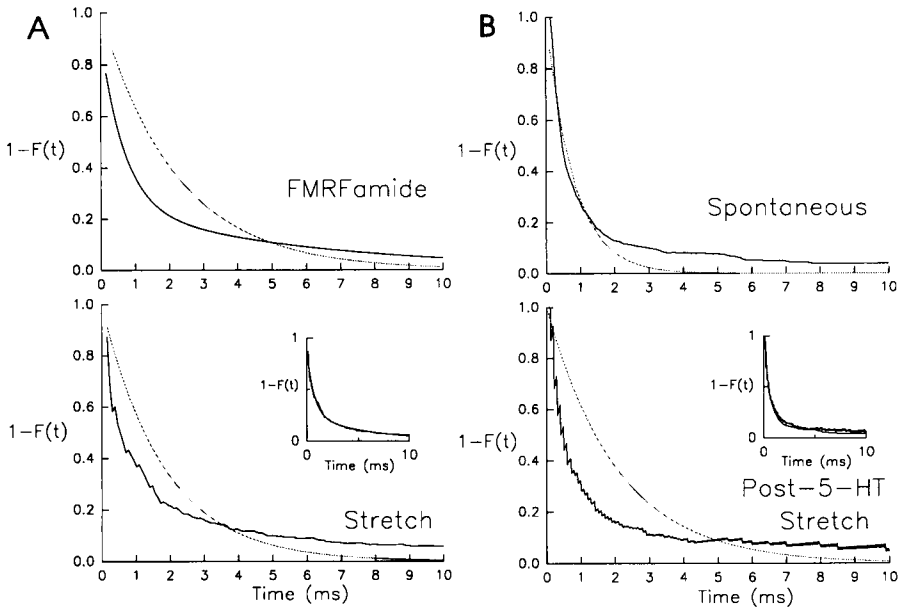

FIGURE 10 Kinetic comparisons using $F(t)$, as estimated by ADaM. (A) FMRFamide and stretch-activated current events from Patch A of Table 4. The solid line is the estimate for $1 - F(t)$, one minus the estimated cumulative open time distribution derived from the nonmodel-specific analysis by ADaM. (see Appendix for explanation of the sawtoothed nature of the estimate). The single exponential plotted as a broken line has a decay constant equal to the global mean open time, τ_o, for this data (see Table 4), as derived from the goodness of fit test described in (Dabrowski and McDonald, 1992), which simultaneously fits N, P, and τ_o (and hence τ_c). In these patches, the null hypothesis of independent and identical channels is not rejected, so N, P, and τ_o (and τ_c) are used to generate the estimated open time probability distribution function, F, by an algorithm described in (Dabrowski et al., 1990). The difference between the $1 - F(t)$ estimate and the single exponential reflect both the inherent error of the initial fit in the ADaM subroutine and the assumption that the channel activity can be adequately modeled as a first order process. ADaM analysis (see Table 4) indicated that N during both the FMRFamide-induced activity and during stretch was three (P_{open} during stretch and FMRFamide activation were similar). V_p, −80 mV; NAS and 10 TEA in pipette and NAS in bath; suction, −88 mm Hg. (B) Spontaneous and stretch activated current events from Patch B of Table 4. Stretch was applied after 5-HT treatment (which "knocked out" all but one channel), when three of the four channels (see Table 4) that were initially spontaneously active had recovered from 5-HT knock-out. V_p, −100 mV; NAS and 10 TEA in pipette, NAS in bath; suction, −60 mm Hg.

increasing suction had no consistent effect on short time constants, it may be that one region of the channel is responsible for the flickery transitions and that a different region is responsible for tension-sensitive gating. Thermal movements of residues near the selectivity filter, a region evidently unaffected by tension, might for example yield the conductance flickers. Tension-sensitive and fatty acid metabolite-dependent gating, by contrast, might both arise from residues at the cytoplasmic mouth or the protein-bilayer interface.

Like other stretch channels, S-channels remain stretch sensitive in excised patches. Likewise, S-channels in excised patches are directly activatable by an arachidonic acid metabolite in the FMRFamide/lipoxygenase pathway (Buttner et al., 1989). A possibility consistent with the similar kinetic effects of stretch and FMRFamide on the S-channel is that stretch and the metabolite converge on a common gating process. Interestingly, a broad spectrum of free fatty acids and stretch can both activate K channels in smooth muscle (Kirber et al., 1990).

Multiple-Channel Patches versus One Channel Patches

Many cell types, including molluscan neurons contain several stretch channel varieties (Morris, 1993). In low activity multichannel records, contributions from distinct channel types are sometimes evident by inspection of kinetics and/or conductance. Direct detection of heterogeneous contributions to current is not possible at high activity levels. By explicitly testing multichannel data for its binomial character (i.e., testing the assumption that all contributing channels are identical and independent), one checks statistically for heterogeneity. In the patches that we were able to test, stationary stretch-activated data from *Aplysia* neurons usually met the binomial criteria, creating the impression that stretch did not routinely activate a kinetically mixed population of channels. An exception to this generalization is illustrated in Fig. 8 (see also Table 2, Part 2); segment C was stationary but did not meet the binomial criteria of independent and identical channels.

Had suction of cell-attached patches seldom yielded binomial records, the explanation might have been outright channel heterogeneity or, more subtly, kinetic heterogeneity of a single channel type. Apparently it is possible for suction to produce sufficiently isotropic tension in channel-bearing membrane to activate channels identically.

The possibility of heterogeneous contributions to multichannel data also needs checking because S-channels can "spontaneously" switch between low and high probability gating modes Seigelbaum et al., 1982) and because it has

been suggested for piscine SA K channels that stretch-sensitivity itself is phosphorylation-dependent (Medina and Bregestovski, 1991). If individual channels had sufficiently different nonzero P_{open} values for a given stimulus, this would be detected during the ADaM analysis as "nonidentical" channels. One possibility that was not controlled for is that the multichannel analysis is best suited to deal with patches in which channels are not in a low probability gating mode; we may have applied ADaM more often to patches in higher probablility gating modes and the one-channel analysis to patches in lower probability gating modes (i.e., gating as determined by factors other than stretch). This would introduce systematic differences in the kinetics as revealed by one-channel or multichannel analysis.

Siegelbaum and colleagues found that in patches with several spontaneously active S-channels, activity was binomial and that FMRFamide did not alter the number of active channels (N), but changed P_{open} (Belardetti et al., 1987; Seigelbaum et al., 1982). Analysis of our data for stretch-induced channel activity did not yield such a clean story; both parameters were changeable as suction changed. Suction-associated changes in N need to be noted, but are probably not biophysically interesting, in that they probably reflect patch mechanics (pulling of more membrane into the patch or budding off of vesicles for increased and decreased N, respectively) and not channel responses to tension. Unfortunately, this means that for stretch channels, suction-induced NP_{open} changes cannot be safely attributed to P_{open} changes without a rigorous binomial analysis. Stretch-dependent kinetics obtained from one-channel patches (Fig. 5) (assuming the analysis extends to P_{open} values approaching unity) constitute the gold standard. In such patches, by definition, changes in N are not possible, so increases in P_{open} must account for stretch-activation (Morris, 1990). Finding that N can change with stretch in larger multichannel patches is disappointing because one-channel patches are rare, but it does not call into question the one-channel results.

Thus, we have illustrated the use of a set of programs that uses renewal theory as the basis for analysis of data from multichannel patches. Ironically, in doing so, we have shown that the stretch-activated S-channel is not particularly amenable to this sort of analysis. This stems in part from a chronic problem encountered with stretch channels, namely that it is not possible to quantify the intended variable, membrane tension. Related points are that a) suction may produce effects other than tension changes and b) the system may not relax back to its previous condition upon release of suction. This, coupled with the tendency of the S-channel to spontaneously enter different modes, meant that truly stationary data had to be sought carefully (fortunately, ADaM provides a means of doing so). We also found that it was possible to contradict an assumption that has been derived from one-channel patch analysis, namely that the number of channels in the patch remains fixed at various intensities of applied suction. The caveats implicit in these remarks reflect the inherent difficulties of working with either stretch channels or strongly modulated channels, and the S-channel fits both categories. Nevertheless, the multichannel analysis lent support to our thesis that the SA K channel and the S-channel of *Aplysia* mechanosensory neurons are the same entity.

APPENDIX

Notation Comparisons for ADaM

We used a notation appropriate to the channel literature rather than one appropriate to the biostatistics literature. The following list equates our terms to those used by Dabrowski and colleagues in ADaM and in the full mathematical treatment of renewal theory and channel kinetics (Dabrowski, McDonald and Rosler, 1990; Dabrowski and McDonald, 1992).

$$N = c; \quad P_{open} = p; \quad F = F; \quad G = G; \quad \tau_o = \mu_F; \quad \tau_c = \mu_G.$$

Nomenclature for F (and G) functions: the true open (closed) time distribution for the channel under consideration is unknown. $\hat{F}$ is the estimator in the one state case. The other renewal theoretic estimator used in ADaM is the function referred to as the estimated F. Fig. 10 shows estimates (the estimated $\hat{F}$ and the estimated F) obtained from applying each of these estimators to data.

Total current at time $t = X(t)$

Chunk length = u

Levels:

Occupation of current level s during chunk $j = M_{sj}$

Occupation density vector (Fig. 1) = $M_j = \left[\int (j-1) \text{ to } j \right] X(t)\, dt$

and in ADaM,

$\text{occ}(s) = 1/n \sum (j = 1 \text{ to } n) M_{sj}$ (= mean occupation vector)

Downsteps:

Number of downsteps from level s to $s - 1$ during chunk $j = N_{sj}$

Downstep vector (Fig. 1) = $N_j = N(j) - N(j-1)$

and in ADaM,

$\text{dwn}(s) = 1/n \sum (j = 1 \text{ to } n) N_{sj}$ (= mean downstep vector)

Covariance matrix = T_n

Sawtoothed Nature of the Plot for $1 - F(t)$

Both F and G are, by definition, monotonic functions of t, yet their estimates are sawtoothed (as in $1 - F(t)$ plots in Fig. 10). The explanation is that the estimates are computed by the ratio of two numeric integrals–integrals that change values (as functions of t). Because one of these integrals varies smoothly in time, and the other in discrete jumps, the ratio of the two exhibits a sawtoothed pattern. There is no a priori reason to pick the upper or lower envelope of this saw-tooth as the estimate of F (or G). The size of the sawtooth is determined by the amount of data for a particular duration.

We thank D. McDonald for many discussions during the course of this work. This work was supported by research grants from NSERC, Canada, to C. E. M. and to A. R. D.

REFERENCES

Baxter, D. A., and J. H. Byrne. 1990. Differential effects of cAMP and serotonin on membrane current, action potential duration, and excitability

in somata of pleural sensory neurons of *Aplysia*. *J. Neurophysiol.* 64: 978–990.

Bedard, E., and C. E. Morris. 1992. Channels activated by stretch in neurons of a helix snail. *Can. J. Physiol. Pharmacol.* 70:207–213.

Belardetti, F., S. Schacher, E. R. Kandel, and S. A. Siegelbaum. 1986. The growth cones of *Aplysia* sensory neurons: modulation by serotonin of action potential duration and single channel currents. *Proc. Natl. Acad. Sci. USA*. 83:7094–7098.

Belardetti, F., E. R. Kandel, and S. A. Siegelbaum. 1987. Neuronal inhibition by the peptide FMRFamide involves opening of S K channels. *Nature (Lond.)*. 325:153–156.

Buttner, N., S. A. Siegelbaum, and A. Volterra. 1989. Direct modulation of *Aplysia* S-K^+ channels by a 12-lipoxygenase metabolite of arachidonic acid. *Nature (Lond.)*. 342:553–555.

Dabrowski, A. R., D. McDonald, and U. Rosler. 1990. Renewal theory properties of ion channels. *Ann. Statistics*. 18:1091–1115.

Dabrowski, A. R., and D. McDonald. 1992. Statistical analysis of multiple ion channel data. *Ann. Statistics*. 20:1180–1202.

Eaton, D. C., J. M. Russell, and A. M. Brown. 1975. Ionic permeabilities of an *Aplysia* giant neuron. *J. Membr. Biol.* 21:353–374.

Gill, D. R., S. C. Hyde, C. F. Higgins, M. A. Valverde, G. M. Mintenig, and F. V. Sepulveda. 1992. Separation of drug transport and chloride channel functions of the human multidrug resistance P-glycoprotein. *Cell*. 71: 23–32.

Gorman, A. L. F., J. C. Woolum, and M. C. Cornwall. 1982. Selectivity of the Ca^+-activated and light dependent K^+ channels for monovalent cations. *Biophys. J.* 38:319–322.

Guharay, F., and F. Sachs. 1985. Mechanotransducer ion channels in chick skeletal muscle: the effects of extracellular pH. *J. Physiol.* 363:119–134.

Gustin, M., F. Sachs, W. J. Sigurdson, A. Rudnikin, C. Bowman, C. E. Morris, and R. Horn. 1991. Technical comments: single channel mechanosensitive currents. *Science (Washington DC)*. 253:80–802.

Horn, R. 1987. Statistical methods for model discrimination: applications to gating kinetics and permeation of the acetylcholine receptor channel. *Biophys. J.* 51:255–263.

Kirber, M. T., R. W. Ordway, L. H. Clapp, J. V. Walsh, and J. J. Singer. 1990. Both membrane stretch and fatty acids directly activate large conductance, Ca^{2+}-activated K^+ channels in vascular smooth muscle cells. *FEBS Lett.* 297:24–28.

Landaw, E. M., and J. J. Distefano. 1984. Multiexponential, multicompartmental, and noncompartmental modeling. 2. Data analysis and statistical considerations. *Am. J. Physiol.* 246:R665–R667.

Larsen, H. J. 1974. Introduction to Probability Theory and Statistical Inference. 2nd Ed. Wiley and Sons, New York. 313–320.

Lecar, H., and C. E. Morris. 1993. Biophysics of Mechanotransduction. *In* Mechanoreception by the Vascular Wall. G. M. Rubyani, editor. Futura Publishing Co., Inc., Mount Kisco, New York. 1–11.

Lin, S. S., D. Dagan, and L. B. Levitan. 1989. Concanavalin A modulates a potassium channel in cultured *Aplysia* neurons. *Neuron*. 3:95–102.

Martinac, B. 1992. Mechanosensitive ion channels: biophysics and pharmacology. *In* Thermodymamics of Membrane Receptors and Channels. M. B. Jackson, editor. CRC Press, Boca Raton, FL. 327–352.

Medina, I. R., and P. D. Bregestovski. 1991. Sensitivity of stretch-activated K^+ channels changes during cell cleavage cycle and may be regulated by cAMP-regulated protein kinase. *Proc. R. Soc. Lond. B Biol. Sci.* 245: 159–164.

Morris, C. E. 1990. Mechanosensitive ion channels. *J. Membr. Biol.* 113: 93–107.

Morris, C. E. 1992. Are stretch-sensitive channels in molluscan cells and elsewhere physiological mechanotransducers? *Experientia (Basel)*. 48: 852–858.

Morris, C. E. 1993. Stretch-sensitive ion channels. *In* Principles of Cell Physiology and Biophysics. N. Sperelakis, editor. Academic Press. In press.

Morris, C. E., and R. Horn. 1991. Failure to elicit macroscopic mechanosensitive currents anticipated by single channel studies. *Science (Washington DC)*. 251:1246–1249.

Morris, C. E., and W. J. Sigurdson. 1989. Stretch-inactivated ion channels coexist with stretch-activated ion channels. *Science (Washington DC)*. 243:807–809.

Reuter, H., and C. F. Stevens. 1980. Ion conductance and ion selectivity of potassium channels in snail neurones. *J. Membr. Biol.* 57:103–118.

Sackin, H. 1993. Stretch-activated ion channels. *In* Cellular and Molecular Physiology of Cell Volume Regulation. K. Strange, editor. CRC Press, Boca Raton, FL. 215–240.

Shuster, M. J., J. S. Camardo, and S. A. Siegelbaum. 1991. Comparison of the serotonin-sensitive and Ca^{2+}-activated K^+ channels in *Aplysia* sensory neurons. *J. Physiol.* 440:601–621.

Siegelbaum, S. A., J. S. Camardo, and E. R. Kandel. 1982. Serotonin and cAMP close single potassium channels in *Aplysia* sensory neurones. *Nature (Lond.)*. 299:413–417.

Sigurdson, W. J., and C. E. Morris. 1989. Stretch activated ion channels in growth cones of snail neurons. *J. Neurosci.* 9:2801–2808.

Sigurdson, W. J., C. E. Morris, B. L. Brezden, and D. R. Gardner. 1987. Stretch-activation of a K channel in molluscan heart cells. *J. Exp. Biol.* 127:191–209.

Sigworth, F. J., and S. M. Sine. 1987. Data transformations for improved display and fitting of single-channel dwell time histograms. *Biophys. J.* 52:1047–1054.

Sokabe, M., and F. Sachs. 1990. The structure and dynamics of patch-clamped membranes: a study using differential interference contrast light microscopy. *J. Cell. Biol.* 111:599–606.

Vandorpe, D. H., and C. E. Morris. 1992. Stretch-activation of the *Aplysia* S-channel. *J. Membr. Biol.* 127:205–214.